



Mercury Capture by Nano-structured Titanium Dioxide Sorbent during Coal Combustion: Lab-scale to Pilot-scale Studies

Achariya Suriyawong¹, Marina Smallwood¹, Ying Li¹, Ye Zhuang², Pratim Biswas^{1*}

¹ Aerosol and Air Quality Research Laboratory, Department of Energy, Environmental & Chemical Engineering, Box 1180 Washington University in St. Louis, St. Louis, MO 63130

² Energy & Environmental Research Center, University of North Dakota, P.O. Box 9018 Grand Forks, North Dakota 58202

ABSTRACT

The performance of non-carbon based sorbent, titanium dioxide (TiO₂) used with UV irradiation, was evaluated in a laboratory-scale coal combustor and in a slip-stream drawn from a pilot-scale coal combustor. For the laboratory-scale system, mercury capture efficiency peaked at 94% at a sorbent feed rate of 71 mg/m³, with sorbent to coal ratio of 0.0074. For the slip-stream system, mercury capture efficiency achieved 92% at a sorbent feed rate of 622 mg/m³, with sorbent to coal ratio of 0.015. The required sorbent feed rates for both systems were higher than those kinetically estimated from earlier established lab-scale study, indicating the interference of other species in coal combustion flue gas. The sorbent generation technique and injection location significantly affected the physical and chemical properties of the sorbent, and subsequently its performance. Pure anatase generated via a pre-synthesized technique was found to be more effective than a mixture of anatase and rutile crystalline structure generated via in-situ generation and found in commercial TiO₂ (Degussa, P25). This study further revealed that the injection of nano-structured sorbent can be designed to obtain optimal efficiency of capture.

Keywords: Coal combustion; Mercury emission; Nano-structured sorbent; Pollution control; Aerosol modeling.

INTRODUCTION

Mercury emission has been of great concern because of its high toxicity, tendency to bio-accumulate, and difficulty of control. In the United States alone, approximately 120 tons of mercury are released each year from anthropogenic sources (US EPA, 1999; Keeler *et al.*, 2006). Once emitted, mercury can remain airborne and be transported over a long distance before being deposited on the land and water, where it may eventually enter the food chain. Despite a very low concentration of mercury in flue gas (1-30 µg/Nm³), coal combustors are the largest anthropogenic source of mercury emission; they contribute about 40 percent of the total emissions (US EPA, 1999). On March 15, 2005, the United States Environmental Protection Agency (US EPA) issued the Clean Air Mercury Rule (CAMR) to regulate Hg emissions from coal-fired power plants using a cap-and-trade approach. Mercury emission from coal-fired power plants would be reduced from 48 tons per year to 15 tons per year, a reduction of nearly 70% (US EPA, 2005). However, the CAMR was challenged by many States and organizations. On February 8, 2008, the U.S. Court of Appeals for the District of Columbia Circuit vacated the CAMR, and required the US EPA to reconsider the Mercury Rule (Edison Electric Institute, 2008). It is expected that the mercury regulation will be more stringent and the power plants will be required to install Hg control device. As a result, extensive research and development are in progress for control methodologies.

Several methods have been proposed for control of mercury emissions from coal-fired power plants, including sorbent injection, photo-chemical removal, and catalysts for enhanced mercury oxidation (Biswas and Wu, 1998; Biswas *et al.*, 1999;

Brown *et al.*, 2000; Granite and Pennline, 2002). Currently, sorbent injection is the simplest and the most mature approach for gaseous mercury removal. The gaseous mercury contacts the sorbent and adsorbs to its surface; and the sorbent with mercury adsorbed is then collected by existing particle control devices. The sorbent injection technique is simple to control, has minimal impact on plant operation, requires relatively little modification of the utility plants, and has low capital cost. Activated carbon (AC) and activated carbon impregnated with sulfur, chlorine, or iodine, are the most effective sorbents for mercury capture, especially in systems where mercury concentration is high (i.e., municipal waste incinerators). They provide high surface area, approximately 300 m²/g, for mercury oxidation and adsorption. However, their application to mercury capture in coal-fired power plants is limited mainly because of their low capacity at elevated temperatures and problems with flyash disposal (Scotto *et al.*, 1994).

A number of researchers have therefore proposed the use of inorganic sorbents, such as titanium-, calcium- and iron-based sorbents, for mercury capture (Pavlish *et al.*, 2003; Zhuang *et al.*, 2007). Nano-structured titanium dioxide (TiO₂) used with ultraviolet (UV) irradiation is one of the promising technologies for mercury capture (Wu *et al.*, 1998; Lee *et al.*, 2004; Potaniak *et al.*, 2004; Lee *et al.*, 2006). In their laboratory-scale studies, Wu *et al.* (1998) demonstrated mercury capture efficiency of in-situ generated nano-structured TiO₂ with UV light was greater than 98 percent. Nano-structured TiO₂ is the agglomerate of nanometer-sized primary particles, which provides a very high external surface area for adsorption, compared to spherical particles of the same volume. This external surface area is the key parameter governing the efficiency of the sorbent. Mercury capture using the TiO₂ with UV irradiation occurs in a two-step process, as shown in Fig. 1: photocatalytic activation of TiO₂ agglomerates, followed by mercury oxidation and adsorption. Photocatalytic activation occurs when TiO₂ agglomerates are exposed to UV radiation; the highly reactive hydroxyl radicals

* Corresponding author. Tel.: (314)-935-5482;
Fax: (314)-935-5464
E-mail address: pratim.biswas@wustl.edu

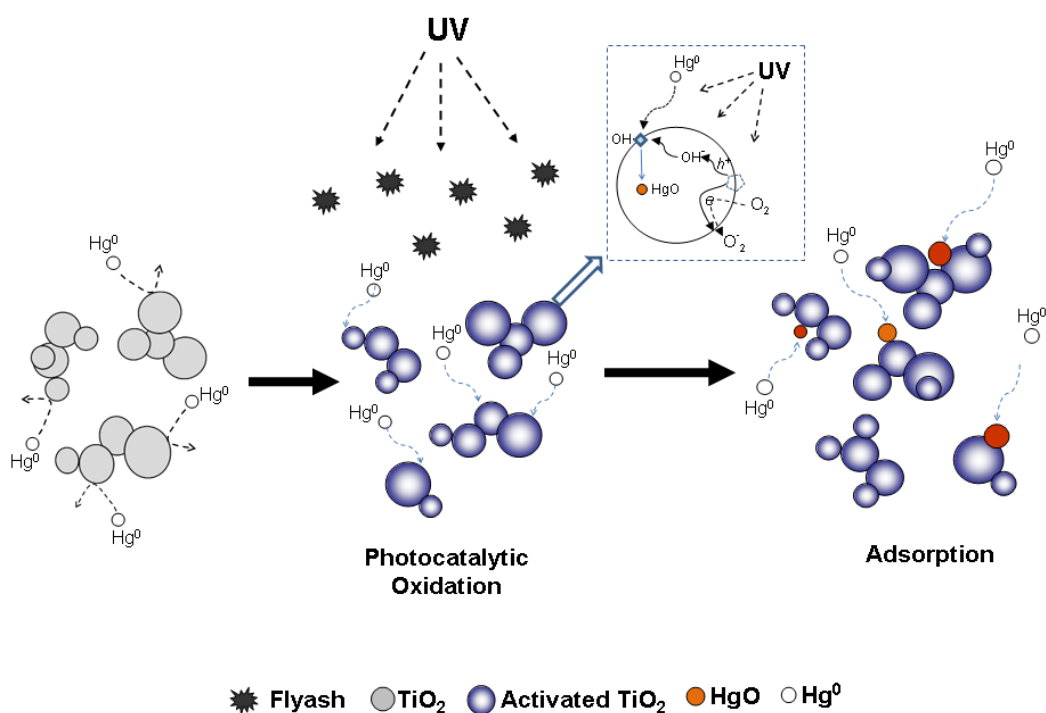


Fig. 1. Mechanistic pathway of Hg capture by TiO_2 with UV irradiation.

(OH) are generated on the surface of the particles, referred as the active surface. Then, gaseous mercury molecules adsorb and are oxidized onto the active surface to form a stable sorbent-mercury complex ($\text{HgO-TiO}_2(\text{complex})$). The $\text{HgO-TiO}_2(\text{complex})$ is retained on the particle surface; therefore, it can be removed from the gas stream by typical particulate control devices. A number of studies have been dedicated to identify the key parameters governing the performance of this control technique. Lee *et al.* (2004) reported a linear dependence of Hg oxidation on the surface area for a differential bed reactor and an aerosol flow reactor. Lee *et al.* (2006) evaluated the effect of different light sources and wavelengths on mercury removal efficiency by TiO_2 : the efficiency was highest at 365 nm. Rodríguez *et al.* (2004) and Li and Wu (2006) studied the role of moisture on mercury oxidation and capture. Mercury oxidation was promoted by low water vapor concentrations (700-1800 ppm_v); however, it was inhibited by the competitive adsorption of mercury and moisture at high moisture conditions (greater than 2,000 ppm_v). In addition to the gas phase mechanistic and kinetic studies, sequential leaching from TiO_2 after mercury capture was also evaluated. Mercury was found to be bound very strongly to the sorbent as a stable sorbent-mercury complex. Thus, the sorbent-fly ash mix could be readily disposed or re-used (Noel *et al.*, 2007).

While TiO_2 with UV irradiation has been successfully demonstrated in many laboratory-scale experiments using simulated flue gas, before this sorbent can be selected for full-scale application, its effectiveness in coal combustion systems needs to be evaluated. Coal combustion systems pose several challenges to the performance of sorbents, such as the interference of fly ash and other flue gas constituents, and short residence time of flue gas in the system. To date, there has been no study on the nano-structured TiO_2 with UV irradiation for mercury capture in coal combustion systems.

Nano-structured TiO_2 sorbent can be generated by several methods. In-situ oxidation of the sorbent precursor is the simplest technique that provides very high surface area per unit mass. At high temperature, the vapor precursor decomposes and forms molecular-sized particles. These particles undergo aerosol growth

dynamics, such as coagulation and sintering, in the combustion system, resulting in agglomerates of molecular- or nanometer-sized particles. The term sintering in this paper refers to coalescence of connected particles through neck formation by solid-state diffusion, which results in a reduction of surface area and agglomerate size. Understanding the evolution of sorbent particles in the system will allow optimal sorbent injection strategy to be developed at the minimal cost.

In this study, the effectiveness of TiO_2 with UV irradiation for mercury capture was investigated in two systems at different scales, (1) a laboratory-scale coal combustor, and (2) a slip-stream system drawn from a pilot scale coal combustor system. The importance of sorbent injection strategy, including sorbent generation and injection locations, on the effectiveness and efficiency of the sorbent was also highlighted. The results of this study allow us to effectively design the sorbent for higher efficiency.

METHODOLOGY

Test Plan

The overall objective is to evaluate the effectiveness of TiO_2 with UV irradiation for mercury capture from coal combustion systems. The test plan was designed as outlined in Table 1. In Set I of the test, experiments were conducted in a laboratory-scale coal combustion system to determine the role of sorbent injection strategy, including the form of the injected sorbent and the sorbent injection location, on the effectiveness and efficiency of the sorbent for mercury capture. The effects of these variables on the properties of the sorbent were also evaluated. In Set II, the best sorbent injection strategy obtained from Set I was tested with the flue gas from a pilot-scale coal combustion system, using a slip-stream. The slip-stream system allowed us to evaluate the effectiveness of the sorbent in flue gas similar to that of full-scale coal combustion exhaust, while the key parameters influencing the effectiveness of the sorbent, i.e., residence time and light distribution, were still under proper control. The initial feed rate of TiO_2 was estimated from the kinetic expression developed by Lee

Table 1. Summary of experiments and simulations conducted.

Set	test	TiO ₂ Generation Technique	Injection Location	Selected TiO ₂ feed rate (mg/m ³)	TiO ₂ feed rate (mg/m ³) Kinetically estimated	[Hg] (μg/m ³)
I (Lab-scale System)	1	in-situ generated	Coal combustor	14.2, 28.4, 71	60.0	1.0 ± 0.1
	2	pre-synthesis	After combustor	14.2, 28.4, 71		
	3	Degussa P25	Coal combustor	10, 50, 100		
II (Slip-stream System)	4	pre-synthesis	Before photo-reactor	114, 228, 622	160.0	2.5 ± 0.2
	5	Degussa P25		3,000		
III (Simulation in the Pilot-scale System)	6	in-situ generated	Coal combustor, After combustor, After heat exchanger	1,000		
	7	Degussa P25				

et al. (2004) for each system. The designed TiO₂ feed rates are shown in Table 1. In Set III, a modeling study was performed on the pilot-scale system to evaluate the effects of sorbent injection strategy, i.e., the forms of sorbent injected and the sorbent injection location, on the properties of the sorbent, including the surface area per unit mass and the eventual particle size at the exit of the combustion system.

Sorbent Used

Three types of TiO₂ particles were tested in this study: TiO₂ generated in-situ by oxidation of its precursor, pre-synthesized TiO₂, and commercial TiO₂ (Degussa-Hüls, TiO₂ P25). A vapor phase precursor, titanium tetra-isopropoxide (TTIP, Ti[OCH(CH₃)₂]₄; 97% Aldrich), was used for the in-situ synthesized TiO₂ and the production of pre-synthesized TiO₂. For the in-situ generated TiO₂, TTIP was injected into the coal combustor, decomposed, and formed TiO₂ particles. For the pre-synthesized TiO₂, TTIP was injected into a small tubular furnace (Thermolyne, Type 2110) with an alumina reactor (ID = 1.9 cm; L = 50 cm), for decomposition and formation of TiO₂ particles. These particles could be introduced into the combustion system at low temperature locations. The TiO₂ particles formed by these two techniques provided higher external surface area for adsorption than did the bulk sorbent. The sorbent injection techniques applied for each system are summarized in Table 1, and the sorbent injection locations for each system are shown in Fig. 2A, and 2B, respectively. TTIP was introduced by into the system in the vapor phase using an impinger (bubbler nozzle with a sintered glass filter) with nitrogen as a carrier gas. The TiO₂ feed rates were varied by changing the N₂ flow rate and bubbler temperature. To minimize nucleation of TTIP, the tubing using heating tape. For TiO₂ injection, a fluidized bed solid feeding system was used.

Sorbent Characterization Methods

The synthesized TiO₂ particles generated in the laboratory-scale and slip-stream systems were well characterized using different analytical techniques. During the synthesis process, the particle mobility size distributions were measured online using a real time scanning mobility particle spectrometry (SMPS) including a differential mobility analyzer (DMA, Model 3081, TSI Inc.) and a condensation particle counter (CPC 3022, TSI Inc.). After particle collection on the filter paper, the X-ray diffraction (XRD) patterns were measured using a Rigaku, Geigerflex D-MAX/A Diffractometer with Cu-K α radiation, $\lambda = 1.5418 \text{ \AA}$. Based on the diffraction patterns the weight fractions of each phase for mixed anatase and rutile samples were calculated. BET isotherms (Autosorb-1, Quantachrome) were used to measure the specific surface area of the nanoparticles with nitrogen adsorption at 77K.

Mercury Measurement Methods

Gaseous mercury in our laboratory-scale study was measured using a mercury sampling train and technique based on the method developed by Hedrick *et al.* (2001). The sampling train consisted of the following five impinger solutions: two impingers of 1.0 M tris-buffer and EDTA for capture of oxidized mercury, one impinger of 10% hydrogen peroxide and 2% nitric acid for oxidizing and capture of elemental mercury, and two impingers of 0.05 M potassium iodide and 2% hydrochloric acid for capture of elemental mercury. The impinger solutions were analyzed by inductively coupled plasma mass spectrometry (ICP-MS) to determine the elemental and oxidized fractions of mercury in the exhaust gas. All experiments were repeated at least three times to obtain statistically significant results.

In the slip stream tests, a continuous mercury measurement (Tekran model 2537A, Toronto, Canada) was done with a wet conversion system. The wet conditioning unit consisted of two impingers containing chemical solutions for conditioning the sample gas for elemental mercury and total mercury measurements. The elemental mercury impinger contained a solution of 1.0 M potassium chloride (KCl) and 1.0 M sodium hydroxide (NaOH). The KCl captured oxidized mercury, and the NaOH captured SO₂. The total mercury impinger contained a solution of 2% stannous chloride (SnCl₂) and 1 M NaOH. The SnCl₂ reduced the oxidized mercury in order to obtain a total mercury measurement. To avoid any residual buildup in the impinger system, fresh solutions were continuously fed to the impingers about 1.5 mL/min by using a peristaltic pump.

Experimental Setup

The laboratory-scale coal combustor, the slip-stream system, and the pilot-scale coal combustor system are described in detail below.

Laboratory-scale Coal Combustion System

The laboratory-scale experimental setup is shown in Fig. 2A and consists of a coal feeding system, a tubular furnace (Lindberg/Blue, Model HTF55342C, T_{max} = 1200°C, Thermolectron Corporation, USA) with an alumina reactor tube (5.72 cm inside diameter and 121.92 cm long), sorbent injection systems, and measuring systems. Pulverized Powder River Basin (PRB) sub-bituminous coal, with a mean particle size of 50 μm was introduced into the heated alumina tubular reactor by a fluidized bed coal feeder at a rate of 1.0 g/hr. The furnace temperature was maintained at 1200°C with excess air (1.75 L/min air feed rate) to ensure complete combustion. Following the reactor, the exhaust passed through a photochemical reactor irradiated with UV light, and a filter. The photochemical reactor had a diameter of 5.7 cm and a length of 59 cm; at a flow rate of

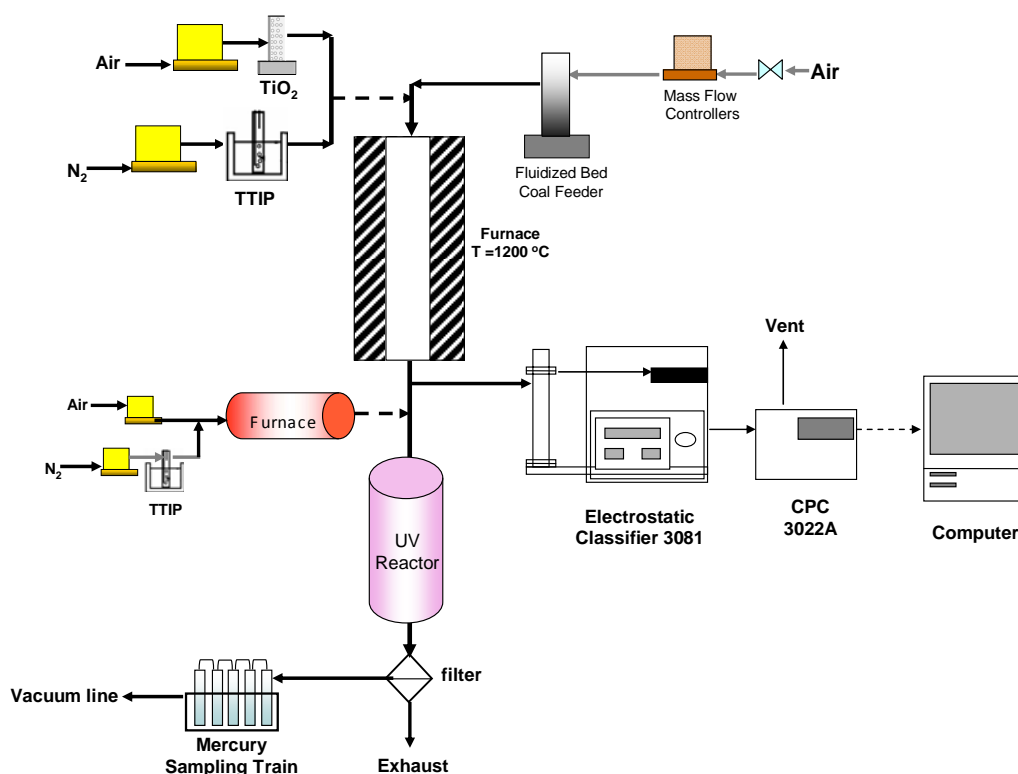


Fig. 2A. Schematic diagram of a laboratory-scale experimental study.

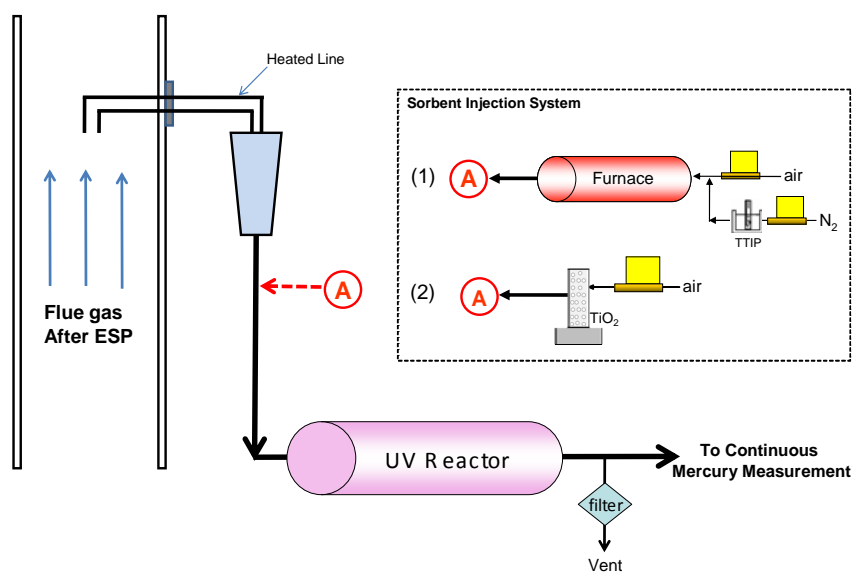


Fig. 2B. Schematic diagrams of a slip-stream system.

1.75 L/min this corresponded to a residence time of 52 s in the photochemical reactor cell. The UV lamp, manufactured by Spectronics Corporation (Spectroline Model XX-40 Longwave UV-365 nm), was 122 cm long, with an intensity of $1850 \mu\text{W}/\text{cm}^2$ at a distance of 8 cm. Following the filter, 1.0 L/min of the exhaust passed through an impinger sampling train while the remainder of the flow was vented to the fume hood.

Powder River Basin subbituminous coal (PRB) used in this study was supplied by AmerenUE, St. Louis, MO. This coal came from Wyodak-Anderson seam, North Antelope/Rochelle mine, Gillette, WY. This mine supplied approximately 91.5 million tons of

compliance coal to 60 power plants throughout the United States in 2007. The proximate and ultimate analyses of the coal are presented in Table 2.

Slip-stream System

The slip-stream system was fed from the pilot system. The system allowed proper control of the key parameters, including UV light intensity and residence time under UV light. The slip-stream was drawn from the outlet of the electrostatic precipitator (ESP) of the combustion system. The slip-stream experimental setup, shown in Fig. 2B, consisted of sorbent

Table 2. Proximate and ultimate analyses of PRB coal using in the lab-scale and pilot-scale coal combustion systems.

Coal	Lab-scaled System	Pilot-scale System
Proximate Analysis (%wt)		
Volatile Matter ^a	48.3	46.5
Fixed Carbon ^a	42.9	41.2
Ash ^a	8.0	7.4
Moisture ^b	27.7	19.0
Low Heating Value ^a (MJ/kg)	28.04	27.92
Ultimate Analysis (%wt)^a		
Carbon	67.3	60.6
Nitrogen	0.96	0.66
Hydrogen	4.58	5.57
Oxygen	19.9	26.9
Sulfur	0.57	0.36
Chlorine	0.01	0.008
Mercury (ppm _{wt})	0.08	0.051

Note: a: as dry weight basis; b: as received weight basis.

injection systems, a photochemical reactor with UV irradiation, and a mercury measurement system. Two types of TiO₂ particles were tested in this system: pre-synthesized TiO₂, and commercial TiO₂. For the pre-synthesized TiO₂, TTIP was injected into a small tubular furnace for decomposition and formation of TiO₂ particles. The furnace temperature was maintained at 900°C to ensure complete decomposition of the sorbent precursor. Following the furnace, combustion flue gas, at the flow rate of 3.0 L/min, was mixed with a 2.0 L/min TiO₂ particle-laden carrier gas before entering a photochemical reactor irradiated with UV light. For the injection of commercial TiO₂, TiO₂ particle-laden air by-passed the furnace and was added into the combustion flue gas prior to entering a photochemical reactor. At a flow rate of 5 L/min, this corresponded to a residence time of 18.2 s in the reactor. The temperature in the reactor, as well as the tubing from the sampling location and leading to the furnace and the photochemical reactor were also held at 80°C using heating tape. The reactor was operated at the same condition as that in the laboratory-scale study. After the reactor, 2.0 L/min of flue gas was drawn to a continuous mercury measurement system and the remaining gas was vented to the exhaust.

Pilot-scale Coal Combustion System

At the Energy and Environmental Research Center (EERC), Grand Forks, ND, a pilot-scale test was conducted, using a 550,000 Btu/hr pulverized coal-fired unit. This system was designed to obtain combustion conditions and characteristics, i.e., a time-temperature profile, similar to that produced in a full-scale utility. A schematic of the system is shown in Fig. 2C. The system consists of a combustor, cold-water annular heat exchangers, an air heat exchanger, a single-wire tubular electrostatic precipitator (ESP), and a bag house. Pulverized Powder River Basin (PRB) sub-bituminous coal, obtained from the same mine as that used in a laboratory-scale coal combustion study, was introduced with the primary air stream into the combustor at a feed rate of 28 kg/hr via a screw feeder and eductor. Based on the superficial gas velocity, the mean residence time in the combustor was approximately 3 seconds.

The temperature in the coal combustor was approximately 1600°C. After exiting the combustor, combustion flue gas at a flow rate of 340 m³/hr at 1000°C passed through a water heat exchanger and an air heat exchanger, which brought the flue gas temperature down to approximately 150°C before it entered the ESP and the fabric filter. The total residence time of the flue gas in the pilot-scale combustion system was approximately 32 s.

Modeling Approach

A bi-modal model developed by Jeong and Choi (2003) was employed to understand the growth dynamic of sorbent particles in the combustion systems. This model accounted for the morphology of the aggregates in a dynamic manner, which gave a more accurate prediction of the surface area and the collision rates of growth than the traditional models that assumed spherical particles. The detailed description of the model can be found elsewhere (Jeong and Choi, 2003; Kim *et al.*, 2009). In the simulations, TiO₂ is introduced into the system in two forms: as a vapor phase precursor, TTIP, and as commercial TiO₂. For the precursor feed, the initial size of the sorbent is its monomer size (4.02 Å) (Jeong *et al.*, 2006). In the Set III study, a modeling study was performed for the pilot-scaled system to evaluate the effects of sorbent injection strategy. According to the structure of the pilot-scale facility, three sorbent injection locations were selected: (1) at the combustor, (2) after the combustor, and (3) after heat exchanger, as shown in Fig. 2C. The temperatures at these locations are 1600, 1100, and 500°C, respectively. All simulations were performed until the flue gas entered the ESP.

RESULTS AND DISCUSSION

Mercury Capture in the Laboratory-scale Coal Combustion System

The mercury capture efficiencies of different injection strategies for an inlet mercury concentration of $1.0 \pm 0.2 \mu\text{g}/\text{m}^3$ are shown in Fig. 3. An average of $0.18 \mu\text{g}/\text{m}^3$ (18%) was oxidized mercury, and $0.95 \mu\text{g}/\text{m}^3$ (82%) was elemental mercury. From the proximate analysis of this PRB coal, shown in Table 2, this type of coal had low sulfur and chlorine contents, resulting in limiting the extent of mercury oxidation. The elemental composition analysis indicated that all the mercury from the coal was released into the gas phase. The sorbent feed rate selected in this set of experiments ranged between 14.2 to 71.0 mg/m³ (0.886 lb/MMacf to 4.43 lb/MMacf). According to the kinetic expression (Lee *et al.*, 2004), the required feed rates of TiO₂ was approximately 60.0 mg/m³ at 90% removal efficiency. This designed feed rate resulted in mercury-to-TiO₂ of 0.016 mg Hg per gram of TiO₂. Three sorbent injection strategies were evaluated in this lab-scale study. The first injection strategy was the in-situ generated nano-structured TiO₂. The sorbent particles were generated from the decomposition of vapor phase precursor (titanium tetra-isopropoxide, TTIP, Ti[OCH(CH₃)₂]₄), inside the coal combustion system. In the second injection strategy, pre-synthesized TiO₂ agglomerates

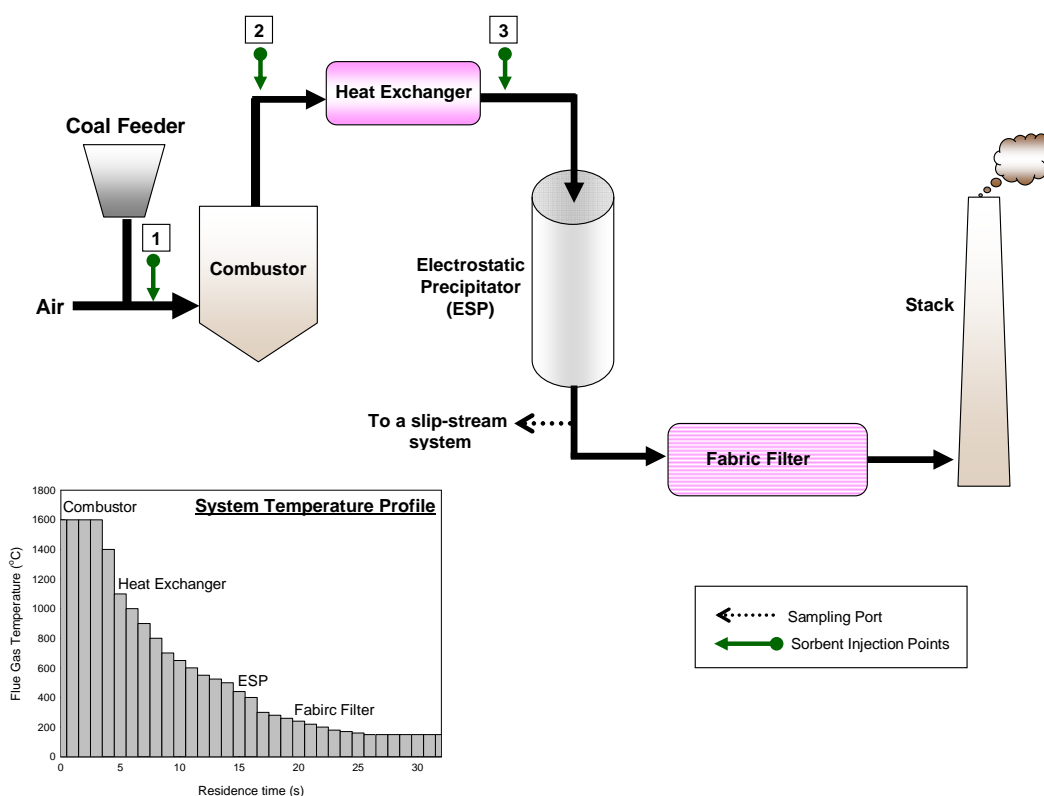


Fig. 2C. Mercury capture in a lab-scale coal combustion study using different sorbent injection strategy.

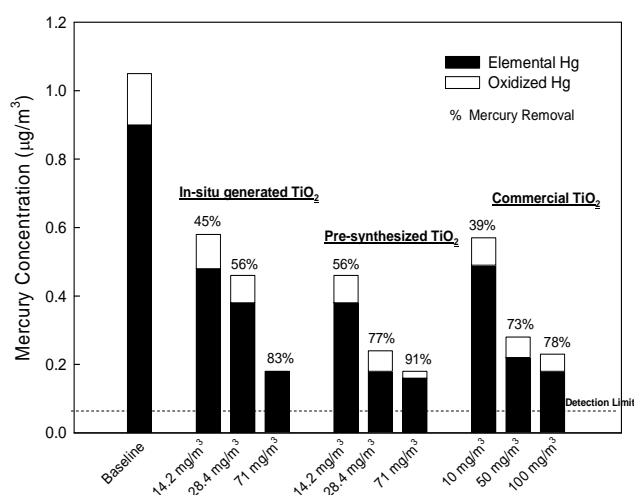


Fig. 3. Mercury capture in a lab-scale coal combustion study using different sorbent injection strategy.

were generated in a small furnace using TTIP, and then introduced to the combustion exhaust gas upstream of the photochemical reactor. In the third injection strategy, commercial TiO₂ particles were introduced into the combustion system with coal.

Substantial reductions in mercury emissions in the exhaust were observed for all three sorbent injection strategies, as presented in Fig. 3. The highest reduction, 91%, was obtained from sorbent injection strategy 2 (the pre-synthesized TiO₂), followed by 83% from injection strategy 1 (in-situ generated TiO₂), and 78% from injection strategy 3 (commercial TiO₂). Experimental results demonstrated that for all of the three sorbent injection strategies the amount of sorbent required to achieve 90% mercury removal

was higher than that estimated from the kinetic calculation (60.0 mg/m³). The difference was attributed to the potential interference of flyash, since the effectiveness of TiO₂ sorbent depends on the intensity of the UV light (Lee *et al.*, 2004). The presence of flyash could hinder the photocatalytic activation of TiO₂ particles. The flyash loading in this lab-scale coal combustion was approximately 760 mg/m³. The potential interference of other compositions in flue gas would be negligible since the coal-to-air mass ratio in the laboratory-scale coal combustion system (1:95) was low compared to that in the pilot and full-scale coal combustion systems (ranging between 1:5 and 1:7).

Among the three sorbent injection strategies, the pre-synthesized TiO₂ exhibited the highest mercury removal for all feed rates. This was attributed to the high surface area for adsorption and to the highly anatase crystalline structure of the TiO₂. The properties of TiO₂ agglomerates generated from different techniques are shown in Table 3 and the agglomerate size distributions of the in-situ generated TiO₂ and the pre-synthesized TiO₂ are shown in Fig. 4. For all sorbent precursor feed rates, the pre-synthesized TiO₂ exhibited a larger geometric mean agglomerated size than that of the in-situ generated TiO₂. The total surface area of the pre-synthesized TiO₂ agglomerates was higher than that of the in-situ generated for all feed rates of sorbent precursor, leading to higher mercury capture. The differences in the surface area were attributed to the sintering effect. The in-situ generated TiO₂ particles were exposed to higher temperature (1200°C) over a much longer residence time than those in the pre-synthesized furnace and the residence time were 900°C and 2 s, respectively). Hence, a higher surface area reduction was observed.

The performance of the sorbents also depends on its chemical (crystalline phase) properties. The TiO₂ with anatase crystal structure exhibits more photocatalytic activity than the rutile phase (Kim *et al.*, 2001), and thus is preferred in mercury capture. All nano-structured TiO₂ prepared in this study have anatase crystal

Table 3. Properties of TiO₂ particles generated from different techniques.

Combustion system	Sorbent Generation Technique	TiO ₂ feed rate (mg/m ³)	Crystal phase	SA ^a (m ² /g)	D ^b (nm)
Lab-scale	In-situ generated	14.2, 28.4, 71	90%A/ 10%R	60.4, 58.6, 57.8	32.2, 37.2, 42.9
	pre-synthesis	14.2, 28.4, 71	100%A	65.5, 63.6, 60.8	44.5, 55.2, 68.5
	Degussa P25*	10, 50, 100	80%A/ 20%R	52	-
	Degussa P25**	10, 50, 100	72%A/ 28%R	48.0, 46.3, 45.0	40.4, 65.8, 80.2
Slip-stream	pre-synthesis	114, 228, 622	100%A	63.5, 62.6, 60.4	80.5, 105.8, 121.3
	Degussa P25*	3,000	80%A/ 20%R	52	-

Note: A: Anatase Phase, R: Rutile Phase

* measured before introduction into coal combustor

** measured after coal combustor

^a specific surface area of particles measured by N₂ adsorption (BET)

^b mobility agglomerate size determined by a scanning mobility particle spectrometry

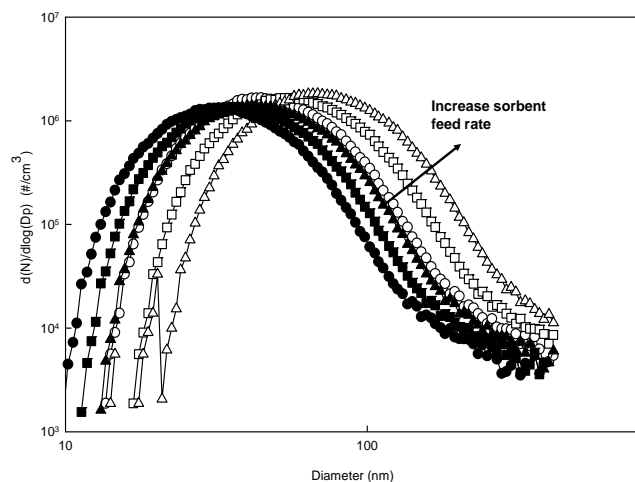


Fig. 4. Particle size distribution of TiO₂ agglomerates generated by different techniques. Legend: Pre-synthesized: \circ -14.2 mg/m³; \square -28.4 mg/m³; \triangle -71 mg/m³. In-situ generated: \bullet -14.2 mg/m³; \blacksquare -28.4 mg/m³; \blacktriangle -71 mg/m³.

structure. The XRD spectra of TiO₂ agglomerates synthesized by different techniques and commercial Degussa TiO₂ are shown in Fig. 5, along with the standard peak distributions of anatase and rutile. The crystalline structure of the in-situ generated TiO₂ was 90% anatase and 10% rutile, while 100% anatase was found in the pre-synthesized TiO₂. For Degussa TiO₂, the crystalline structure was altered from 80% to 72% anatase and 20% to 28% rutile after it passed through the combustor. Anatase, a meta-stable crystal form, tends to transform into the thermodynamically stable polymorph, rutile, when the particles are exposed to high temperature for a long period (Yan *et al.*, 2005). Both in-situ generated TiO₂ particles and Degussa TiO₂ particles encountered higher temperature in the coal combustor (1200°C), with a longer residence time (~1 min) than those that had undergone the pre-synthesized process, resulting in small fraction of rutile crystalline formed.

The results obtained from this set of experiments indicate that the sorbent synthesis technique and the sorbent injection location significantly affect both the physical and chemical properties of the sorbent, and subsequently its performance. These findings can guide effective and efficient designs for mercury removal.

Mercury Capture in the Slip-stream Coal Combustion System

The measured mercury concentrations from the slip-stream drawn from the pilot-scale coal combustion system are shown in Fig. 6. The mercury concentration was slightly lower than that in

actual flue gas because the flue gas was diluted with TiO₂ laden carrier gas. Most of the mercury was in elemental form, which was consistent with the findings of our laboratory-scale study. Because of the high ash loading in flue gas upstream of the ESP, approximately 2.5 g/m³, UV light distribution in the photocatalytic reactor was essentially prevented, and the slip-stream was drawn from the outlet of the ESP. The pre-synthesized TiO₂ and commercial Degussa TiO₂ were evaluated in this study. Both types of TiO₂ sorbent showed a substantial reduction of gaseous mercury. According to the kinetic expression from Lee *et al.* (2004), the designed feed rates of TiO₂ were approximately 160 mg/m³ at 90% removal. The selected injection rates of pre-synthesized TiO₂ were 114, 228, and 622 mg/m³ (7.11 lb/MMacf to 38.8 lb/MMacf), resulting in mercury reductions of 13%, 46%, and 90%, respectively. The differences in the required feed rate between kinetic estimation and experimental results were attributed to the interference of flue gas constituents. Since flue gas was drawn from the outlet of the ESP, the potential interference of flyash was negligible. One of the potential interferences is moisture. Moisture is known to be the important parameter effecting both photocatalytic oxidation and adsorption. Moisture is necessary for generating hydroxyl radicals, the active reagents for photocatalytic oxidation. However, high moisture reduces adsorption capacity by occupying active sites on the TiO₂ particle, and thus its efficiency (Pitoniak *et al.*, 2004; Li and Wu, 2006). Moisture concentration in the coal combustion flue gas, approximately 8% by volume, was much higher than the optimal concentration (700-1800 ppm.) where both adsorption and photocatalytic oxidation can occur (Rodriguez *et al.*, 2004). As a result, mercury oxidation rate was decreased. Furthermore, in coal combustion flue gas, other metallic species are also present, which may result in the competitive occupancy of the available adsorption sites. For commercial Degussa TiO₂, the required feed rate to achieve 93% mercury reduction was approximately 3,000 mg/m³. The pre-synthesized TiO₂ demonstrated higher efficiency than commercial TiO₂ because it exhibited pure anatase crystal structure and higher available surface area for adsorption, which were consistent with the study in the laboratory-scale coal combustion system.

Sorbent Injection Strategy the Pilot-scale Coal Combustion System

The previous sections have shown that the surface area exposed to UV light significantly affects the efficiency of the sorbent. To effectively prevent mercury emission into the atmosphere, the spent sorbents have to be captured by a particulate control device. The large agglomerate size would result in the most effective capture in an existing particle control device, such as ESP (Suriyawong *et al.*, 2008). In addition, as cost is important, minimal sorbent loading while achieving good removal efficiency

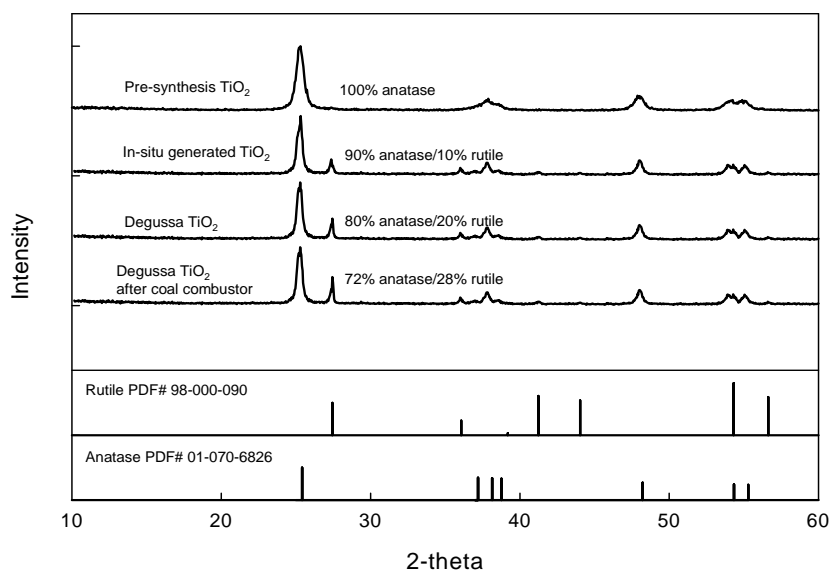


Fig. 5. The XRD pattern of TiO₂ particles synthesized by different techniques.

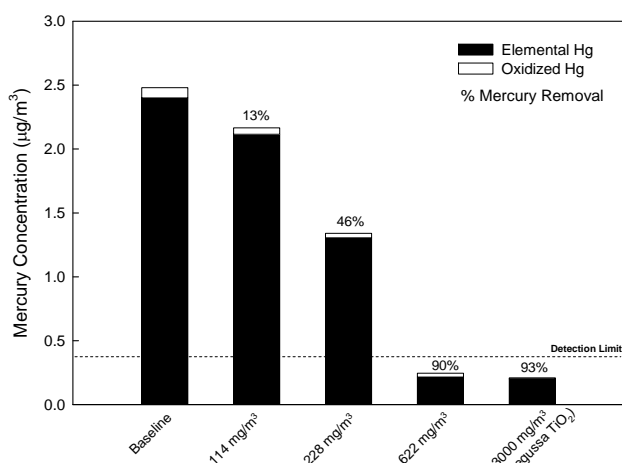


Fig. 6. Mercury capture in a slip-stream study using pre-synthesized TiO₂ agglomerates and commercial TiO₂ (Degussa P25).

is always preferred. Hence, it is important to develop the sorbent injection strategy to effectively and efficiently implement nano-structured TiO₂ with UV irradiation for Hg capture. A model simulation was employed to understand the growth dynamic of the sorbent and to determine the optimal sorbent injection strategy. In the simulations, TiO₂ is introduced into the system in two forms: as a vapor phase precursor, TTIP, a commercial TiO₂. Three sorbent injection locations are selected: (1) at the combustor, (2) after combustor, and (3) after heat exchanger. The temperatures at these locations are 1600, 1100, and 500°C, respectively. All simulations were performed until the flue gas entering an ESP. The key parameters used to determine the best injection strategies are surface area per unit mass and agglomerate size. The results from the simulations are shown in Fig. 7A and 7B. The in-situ generated TiO₂ sorbent exhibits higher surface area per unit mass than that of commercial TiO₂ particles for all injection locations, except at location 1 (at the combustor), where the surface area per unit mass of both types of TiO₂ were the same. The high surface area per unit mass of in-situ generated TiO₂ resulted from the molecular-sized TiO₂ particles in the agglomerates, while the

commercial TiO₂ agglomerates consisted of nanometer-sized particles. The simulation results further demonstrated the importance of sorbent injection location. The in-situ generated TiO₂, injected at location 2, exhibited higher surface area per unit mass than at other injection locations, followed by injection locations 3 and 1. The differences are attributed to decomposition of the vapor precursor and the sintering effect. At location 1, the temperatures of the flue gas are high, resulting in rapid decomposition of the Ti-vapor precursor, formation of TiO₂ particles, and growth by Brownian coagulation forming aggregates of molecular-sized TiO₂ particles. However, due to the high temperature environment, the connected particles sintered into closer to spherical shapes, resulting in a reduction of surface area. The temperature inside the combustor is much higher than that after the combustor; thus, there is higher surface area reduction. The differences in the surface area per unit mass for locations 2, and 3 can be attributed to the effect of temperature on the decomposition and oxidation rates of Ti-vapor-precursor. At location 2, the flue gas temperature is much higher than injection location 3. Hence, there are faster decomposition, particle formation, and sintering rates. As shown in Fig. 7A, the surface area per unit mass of in-situ generated TiO₂ injected at location 2 instantaneously increased after the injection, then decreased due to sintering, and became constant afterwards. At location 3, this parameter gradually increased with the residence time, indicating continuous particle generation in the flue gas.

For the commercial TiO₂ sorbent, the surface area per unit mass was highest at injection location 3. The effect of sintering on the reduction of surface area was also observed only at locations 1 and 2. However, the effect was not as significant as that observed in the in-situ generated process because the required sintering time (τ_s) is proportional to the fourth power of the primary particle size (Kruis *et al.*, 1993). The initial size of the primary particle of commercial TiO₂ was larger than that of the in-situ generated process; thus, less impact was observed. The simulations also showed that at location 1, the in-situ generated sorbent and the commercial TiO₂ resulted in the same surface area per unit mass, indicating that the high temperature and long residence time in the combustor outweighed the effect of primary particle size. The efficiency of the sorbent would be minimized if injected into the combustor.

Another important property of the sorbent for Hg capture is its eventual size at the particulate control device. This parameter indicates the capture effectiveness of the sorbent by particulate

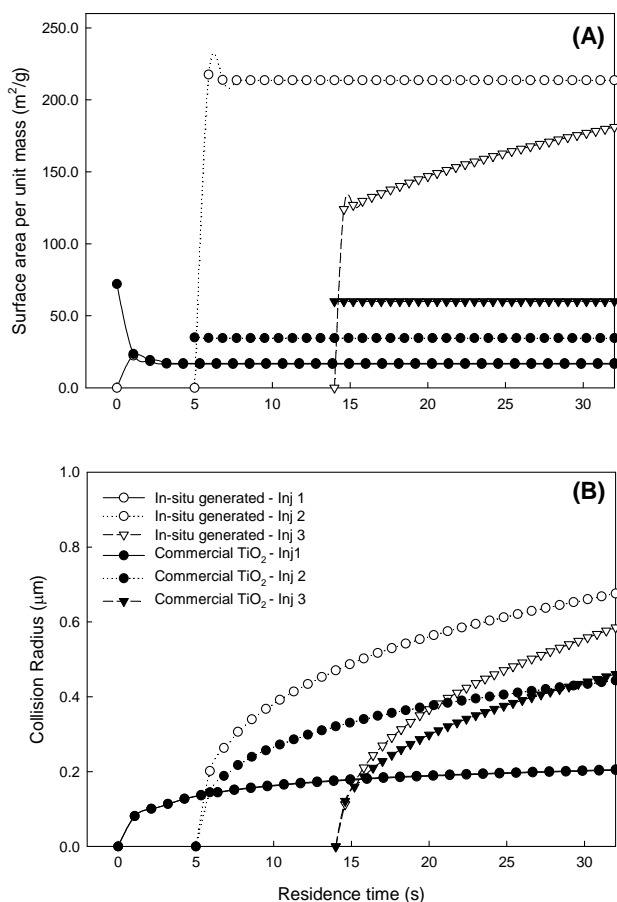


Fig. 7. (A) Evolution of surface area of TiO₂ sorbent generated in-situ and commercial TiO₂ (Degussa, P25) injected at different locations. (B) Evolution of agglomerate size of TiO₂ sorbent generated in-situ and commercial TiO₂ (Degussa, P25) injected at different locations.

control device. Results of the simulations are illustrated in Fig. 7B. The in-situ generated TiO₂ sorbent exhibits larger agglomerate size than that of commercial TiO₂ particles for all injection locations, except at location 1 (at the combustor), where the eventual agglomerate size of both types of TiO₂ were the same. Among the in-situ generated TiO₂, the Ti-precursor injected at location 2 exhibited largest agglomerate size, approximately 0.6 μm at the exit of the combustion system, followed by that at location 3 and 1. The differences are attributed to decomposition of the vapor precursor and the sintering effect, as previously discussed. For commercial TiO₂, the eventual agglomerate size was relatively the same for injection locations 2 and 3, and it was smallest when the sorbent was injected at location 1.

The results of Set III study demonstrated the importance to sorbent injection strategy in the properties of the sorbent. As cost is important, minimal sorbent loading while achieving good removal efficiency is always desired. The sorbent injection needs to be designed, so that the sorbent is effectively and efficiently utilized.

CONCLUSIONS

Titanium dioxide (TiO₂) particle with UV irradiation had been shown to be effective in the capture of gaseous mercury in laboratory-scale experiments using simulated flue gas. This study evaluated the effectiveness and efficiency of the sorbent in two coal combustion systems at different scales, a laboratory-scale

coal combustor and a slip-stream system drawn from a pilot scale coal combustor system. In the laboratory-scale coal combustion system, 94% mercury capture was achieved at a TiO₂ feed rate of 71 mg/m³. In the slip-stream system, 92% mercury capture was achieved at a feed rate of 622 mg/m³. The required sorbent feed rates were higher than those estimated using previously established kinetics expression due to interference by other species present in coal combustion flue gas, e.g., flyash and moisture. The sorbent injection strategy played an important role in the efficiency of the sorbent. Pre-synthesized nano-structured TiO₂ demonstrated the highest efficiency, followed by in-situ generated and commercial TiO₂. The differences in the efficiency were attributed to the properties of the sorbent, including available surface area per unit mass and crystalline structure. This study further demonstrated the importance of sorbent injection strategy, including sorbent generation and injection locations, on the physical properties of the sorbent in a pilot-scale coal combustion system. Sorbent injection should be carefully designed, so that high-surface-area agglomerates result and the sorbent is efficiently utilized. Results of this study also emphasize the importance of the system variables, such as time-temperature profile, coal type, and mercury concentration on the sorbent performance.

Since UV light is also a critical factor governing mercury removal efficiency of the sorbent and the time-scale for the experiments in this study are relatively longer than those in full scale systems (varying from 60 s to 120 s), future studies should focus on designing the distribution of UV light and conducting experiments over relevant time-scales. After effective design of UV light distribution and full-scale studies, nano-structured titanium dioxide with UV irradiation, it could become a promising technology for mercury capture from coal-burning utilities. This inorganic sorbent oxide process does not increase the carbon-content in flyash. The sorbent-flyash mix could be readily disposed or re-used as is done currently since mercury was found to be bound very tightly to the sorbent as established by sequential leachability studies. The TiO₂ sorbent can be efficiently utilized since the sorbent can be injected in high temperature flue gas, which increases contact time of sorbent and mercury. Furthermore, TiO₂ particles can potentially oxidize other hydrocarbon species, i.e. VOCs and PAHs, and suppress nucleation of other metallic species generated in combustion systems.

ACKNOWLEDGEMENTS

The authors thank Mr. Michael Daukoru, Aerosol and Air Quality Research Laboratory, Washington University in St. Louis, St. Louis, MO, for his help with the pilot scale testing. The work was partially supported by grants from the DOE (grant number DE-FGZ6-05NT42531) and Ameren UE., St. Louis, through MODNR (contract number W-0001-06).

REFERENCES

- Biswas, P. and Wu, C.Y. (1998). Control of Toxic Metal Emissions from Combustors Using Sorbents: A Review. *J. Air Waste Manage. Assoc.* 48: 113-127.
- Biswas, P., Senior, C., Chang, R., Vidic, R., Laudal, D. and Brown, T. (1999). Mercury Measurement and Its Control: What We Know, Have Learned, and Need to Further Investigate. *J. Air Waste Manage. Assoc.* 49: 1469-1473.
- Brown, T.D., Smith, D.N., O'Dowd, W.J. and Hargis, R.A. (2000). Control of Mercury Emissions from Coal-fired Power Plants: a Preliminary Cost Assessment and the Next Steps for Accurately Assessing Control Costs. *Fuel Process. Technol.* 65: 311-341.
- Edison Electric Institute (2008). EPA Mercury Regulation. Retrieved January 23, 2009. <http://www.eei.org/ourissues/TheEnvironment/Air/Pages/EPAMercuryRegulation.aspx>.
- Granite, E.J. and Pennline, H.W. (2002). Photochemical Removal

- of Mercury from Flue Gas. *Ind. Eng. Chem. Res.* 41: 5470-5476.
- Hedrick, E., Lee, T.G., Biswas, P. and Zhuang, Y. (2001). The Development of Iodine Based Impinger Solutions for the Efficient Capture of Hg^0 Using Direct Injection Nebulization-Inductively Coupled Plasma Mass Spectrometry Analysis. *Environ. Sci. Technol.* 35: 3764-3773.
- Jeong, I.J. and Choi, M. (2003). A Simple Bimodal Model for the Evolution of Non-Spherical Particles Undergoing Nucleation, Coagulation and Coalescence. *J. Aerosol Sci.* 34: 965-976.
- Jeong, S.K., Kim, S.B., Kim, S.S., Chen, X. and Biswas, P. (2007). Simultaneous Removal of Cd and Pb from Flue Gases Using In-situ Generated Nano-sized Sorbents. *Ind. Eng. Chem. Res.* 13: 1154-1161.
- Keeler, G.J., Landis, M.S., Norris, G.A., Christianson, E.M. and Dvonch, J.T. (2006). Sources of Mercury Wet Deposition in Eastern Ohio, USA. *Environ. Sci. Technol.* 40: 5874-5881.
- Kim, S.B., Kim, S.S. and Biswas, P. (2009). Simple Trimodal Model for Evolution of Multicomponent Aerosol Dynamics. *J. Aerosol Sci.* (submitted).
- Kim, S.J., Lee, E.G., Park, S.D., Jeon, C.J., Cho, Y.H., Rhee, C.K. and Kim, W.W. (2001). Photocatalytic Effects of Rutile Phase TiO_2 Ultrafine Powder with High Specific Surface Area Obtained by a Homogeneous Precipitation Process at Low Temperatures. *J. Sol-Gel Sci. Technol.* 22: 63-74.
- Kruis, F.E., Kusters, K.A. and Pratsinis, S E. (1993). A Simple Model for the Evolution of the Characteristics of Aggregate Particles Undergoing Coagulation and Sintering. *Aerosol Sci. Technol.* 19: 514-526.
- Lee, T.G., Biswas, P. and Hedrick, E. (2004). Overall Kinetics of Heterogeneous Elemental Mercury Reactions on TiO_2 Sorbent Particles with UV Irradiation. *Ind. Eng. Chem. Res.* 43: 1411-1417.
- Lee, Y.G., Park, J.W., Kim, J.H., Min, B.R., Jurng, J., Kim, J. and Lee, T.G. (2004). Comparison of Mercury Removal Efficiency from a Simulated Exhaust Gas by Several Types of TiO_2 under Various Light Sources. *Chem. Lett.* 33: 36-37.
- Li, Y. and Wu, C.Y. (2006). Role of Moisture in Adsorption, Photocatalytic Oxidation, and Reemission of Elemental Mercury on a SiO_2 - TiO_2 Nanocomposite. *Environ. Sci. Technol.* 40: 6444-6448.
- Noel, J.D., Biswas, P. and Giammar, D.E. (2007). Evaluation of a Sequential Extraction Process Used for Determining Mercury Binding Mechanisms to Coal Combustion Byproducts. *J. Air Waste Manage. Assoc.* 57: 856-867.
- Pavlish, J.H., Sondreal, E.A., Mann, M.D., Olson, E.S., Galbreath, K.C., Laudal, D. and Benson, S.A. (2003). Status Review of Mercury Control Options for Coal-fired Power Plants. *Fuel Process Technol.* 82: 89-165.
- Pitoniak, E., Wu, C.Y., Mazyck, D.W., Bonzonco, J.J., Powers, K. and Sigmud, W. (2004). Nano-structured Silica Gel Doped with TiO_2 for Vapor Mercury Capture. *J. Nanopart. Res.* 5: 281-292.
- Rodriguez, S., Almquist, C., Lee, T.G., Furuuchi, M., Hedrick, E. and Biswas, P. (2004). A Mechanistic Model for Mercury Capture with In-situ Generated Titania Particles: Role of Water Vapor. *J. Air Waste Manage. Assoc.* 54: 149-156.
- Scott, M.V., Uberoi, M., Peterson, T.W., Shadman, F. and Wendt, J.O.L. (1994). Metal Capture by Sorbents in Combustion Processes. *Fuel Process Technol.* 39: 357-372.
- Suriyawong, A., Hogan, C.J., Jiang, J. and Biswas, P. (2008). Charged Fraction and Electrostatic Collection of Ultrafine and Submicrometer Particles Formed during O_2 - CO_2 Coal Combustion. *Fuel.* 87: 673-682.
- U.S. Environmental Protection Agency (1999). 1999 National Emission Inventory for Hazardous Air Pollutants. Retrieved November 23, 2004. <http://epa.gov/ttn/chief/net/1999inventory.html>.
- U.S. Environmental Protection Agency (2005). Clean Air Mercury. Retrieved January 23, 2009. <http://www.epa.gov/air/mercuryrule/>
- Wu, C.Y., Lee, T.G., Tyree, G., Arar, E. and Biswas, P., (1998). Capture of Mercury in Combustion Systems by in Situ-generated Titania Particles with UV Irradiation. *Environ. Eng. Sci.* 15: 137-148.
- Yan, M.C., Chen, F., Zhang, J.L. and Anpo, M. (2005). Preparation of Controllable Crystalline Titania and Study on the Photocatalytic Properties. *J. Phys. Chem. B.* 109: 8673-8678.
- Zhuang, Y., Thompson, J.S., Zygarlicke, C.J. and Pavlish, J.H. (2007). Impact of Calcium Chloride Addition on Mercury Transformations and Control in Coal Flue Gas. *Fuel.* 86: 2351-2359.

Received for review, February 9, 2009
Accepted, April 26, 2009